The Astrophysical Journal, 457:604–609, 1996 February 1

VLBI OBSERVATIONS OF THE ULTRACOMPACT RADIO NUCLEUS OF THE GALAXY M81

M. F. Bietenholz,[1] N. Bartel,[1] M. P. Rupen,[2] J. E. Conway,[2] A. J. Beasley,[2] R. A. Sramek,[2] J. D. Romney,[2] M. A. Titus,[3] D. A. Graham,[4] V. I. Altunin,[5] D. L. Jones,[5] A. Rius,[6] T. Venturi,[7] G. Umana,[8] K. W. Weiler,[9] S. D. Van Dyk,[9,10] N. Panagia,[11] W. H. Cannon,[1,12] J. Popelar,[13] and R. J. Davis[14]

Received 1994 October 17; accepted 1995 July 5

ABSTRACT

VLBI observations of the nuclear region of the nearby spiral galaxy M81 reveal the smallest size yet for its core and that of any other extragalactic nucleus: 0.18 mas × 0.07 mas (700 AU × 300 AU) at 22.2 GHz. Images show no brightness structure outside the core region above the sensitivity limit of ∼2% of the peak brightness. The core is slightly asymmetric with its brightness falling off along its major axis toward the northeast. There has been no significant change in the size and orientation since the last VLBI observation of this source in 1981, giving a nominal expansion velocity of -60 ± 60 km s^{-1}. The size varies with observing frequency, with the length of the major axis being proportional to $\nu^{-0.8}$. The apparent position angle is also frequency dependent, and changes by 35° between 22.2 and 2.3 GHz, equivalent to such a change on a length scale from 700 to 4000 AU. These observations exclude a starburst or supernova origin of the core emission and instead argue for the core being an active galactic nucleus, perhaps with a bent jet, and with properties lying between those of Sgr A* and the cores of powerful radio galaxies and quasars.

Subject headings: galaxies: individual (M81) — galaxies: nuclei — radio continuum: galaxies — techniques: interferometric

1. INTRODUCTION

M81 (NGC 3031, 0951+693) is a grand-design spiral at a distance of ∼4 Mpc (Bartel et al. 1994; Freedman et al. 1994; Wheeler et al. 1993) and, together with Centaurus A, is home to the nearest extragalactic compact nucleus.

M81's nucleus appears closely related to the more distant and powerful active galactic nuclei (AGNs) seen in quasars and radio galaxies. The core has a flat or slightly inverted radio spectrum (de Bruyn et al. 1976) with a brightness temperature of $\sim 2 \times 10^{10}$ K (Bartel et al. 1982, hereafter B82), and one sees broad Hα lines (Peimbert & Torres-Peimbert 1981) and high X-ray luminosity ($>10^{40}$ erg s^{-1}, Elvis & Van Speybroeck 1982). However, compared with "normal" AGNs, M81's core is unusual both in that it occurs in a spiral rather than an elliptical galaxy, and in being relatively small and faint. VLBI observations from more than a decade ago (Kellermann et al. 1976, B82) showed that the central source is only 1000–4000 AU across, depending on observing frequency. This small linear size is also consistent with radio-monitoring studies (Crane, Guiffrida, & Carlson 1976) in which variability was found on a timescale of days. The core has a radio luminosity of only $\sim 10^{37.5}$ erg s^{-1} for a frequency range up to 100 GHz, producing a total flux density at, say, 8 GHz of only ∼100 mJy. Therefore, the core of M81 is observable only because it is so nearby; but that nearness also offers an important opportunity for the detailed study of a central engine in a spiral galaxy.

Here we present the results from new VLBI observations of the core of M81 at several frequencies and with a much expanded global array of telescopes. These observations allowed us to (*a*) make images of this nearby nuclear source, (*b*) derive better estimates of its size and orientation, (*c*) determine an extraordinarily small upper bound on the expansion velocity of the source, and (*d*) renew the discussion of the source's physical nature.

2. OBSERVATIONS

We observed the nucleus of M81 as a phase reference source for our VLBI observations of the supernova SN 1993J (Bartel et al. 1994; Rupen et al. 1994). The VLBI observations were made using a global network of between nine and 15 telescopes (see Table 1). We observed at up to four frequencies with the Mk III (Rogers et al. 1983) version A and the VLBA (Napier et al. 1994) VLBI systems in mode B double-speed, which generally gives a bandwidth of 56 MHz. Left-hand circular polarization (IAU convention) was recorded at 22.2 and 5.0 GHz, and right-hand at 14.9 and 8.4 GHz. Here we present the results from the first three sessions, in 1993 April, May, and June. A preliminary presentation of some of these results can be found in Bietenholz et al. (1994).

3. DATA REDUCTION

We correlated the data from a large subarray of antennas, representing 30% of all the data, at Haystack Observatory.

[1] Department of Physics and Astronomy, York University, North York, ON, Canada M3J 1P3.
[2] National Radio Astronomy Observatory, Socorro, NM 87801.
[3] Haystack Observatory, Westford, MA 01886.
[4] Max-Planck-Institut für Radioastronomie, 53121 Bonn, Germany.
[5] Jet Propulsion Laboratory, California Institute of Technology, Pasadena, CA 91109.
[6] Centro de Estudios Avanzados, CSIC, Blanes, 17300 Barcelona, Spain and Laboratorio de Astrofísica Espacial y Física Fundamental, INTA, 28080 Madrid, Spain.
[7] Istituto di Radioastronomia, CNR, 40129 Bologna, Italy.
[8] Istituto di Radioastronomia, CNR, 96017 Noto, Italy.
[9] Code 7215, Naval Research Laboratory, Washington, DC 20375-5351.
[10] Department of Astronomy, University of California, Berkeley, CA 94720.
[11] Space Telescope Science Institute, Baltimore, MD 21218.
[12] Institute for Space and Terrestrial Science, North York, ON, Canada M3J 3K1.
[13] Natural Resources Canada, Ottawa, ON, Canada K1A 0Y3.
[14] Nuffield Radio Astronomy Laboratory, Macclesfield, Cheshire, SK11 9DL, England UK.

TABLE 1

DESCRIPTION OF THE ANTENNAS

Antenna	Code	Diameter (m)	Affiliation and Location
Y27 (VLA)........	Y	130[a]	NRAO, near Socorro, NM
Ef..................	B	100	Max-Planck-Institut für Radioastronomie, Effelsberg, Germany
Ro.................	M	70	NASA-JPL, Robledo, Spain
Go.................	D	70	NASA-JPL, Goldstone, CA
Ag.................	C	46	Institute for Space and Terrestrial Science, York University, Algonquin Park, Ontario, Canada
Gb.................	G	43	NRAO, Green Bank, WV
Mc................	L	32	Istituto di Radioastronomia, CNR, Medicina, Italy
Nt.................	N	32	Istituto di Radioastronomia, CNR, Noto, Italy
Cm................	E	32	NRAL, Cambridge, UK
SC (VLBA).......	V	25	NRAO, St. Croix, VI
HN (VLBA)......	H	25	NRAO, Hancock, NH
NL (VLBA)......	I	25	NRAO, North Liberty, IA
FD (VLBA)......	F	25	NRAO, Fort Davis, TX
PT (VLBA).......	P	25	NRAO, Pie Town, NM
LA (VLBA).......	X	25	NRAO, Los Alamos, NM
KP (VLBA)......	T	25	NRAO, Kitt Peak, AZ
BR (VLBA).......	R	25	NRAO, Brewster, WA
MK (VLBA)......	U	25	NRAO, Mauna Kea, HI

[a] Equivalent diameter of the phased array.

The full data sets will be correlated with the NRAO VLBA processor in Socorro. The self-calibration, imaging, and model fitting of the data were done using NRAO's Astronomical Image Processing System (AIPS) and Caltech's VLBI package including "Difmap" (Shepherd, Pearson, & Taylor 1994).

In Figure 1 we show images of the core of M81 at (*a*) 22.2 and (*b*) 8.4 GHz. The source is clearly elongated along the southwest-northeast axis but only marginally resolved. No other significant emission was found in the maps. Any peak was smaller than 4 times the rms of the background noise, or 2% of the peak flux density of the core in a 10 mas × 10 mas area at 22.2 GHz and a 28 mas × 28 mas area at 8.4 GHz. These areas define the field of view for our integration times, and correspond to 40 beamwidths (FWHM) × 40 beamwidths (FWHM) and ~25% correlation losses at the edges.

Because the images show only simple source structure, we obtained precise values for the size and orientation of the elongated source at each of the frequencies and epochs by model fitting. Since the amplitudes vary smoothly and the closure phases were zero within the errors for most of the antenna triangles and deviated only slightly from zero for the largest ones (Fig. 2), we started by fitting a simple elliptical Gaussian to the *u-v* data. We proceeded as follows: the phases were self-calibrated and constant antenna (amplitude) gain factors determined. For the 22.2 and 8.4 GHz data, amplitudes and phases were coherently averaged into 2 hr bins. This procedure

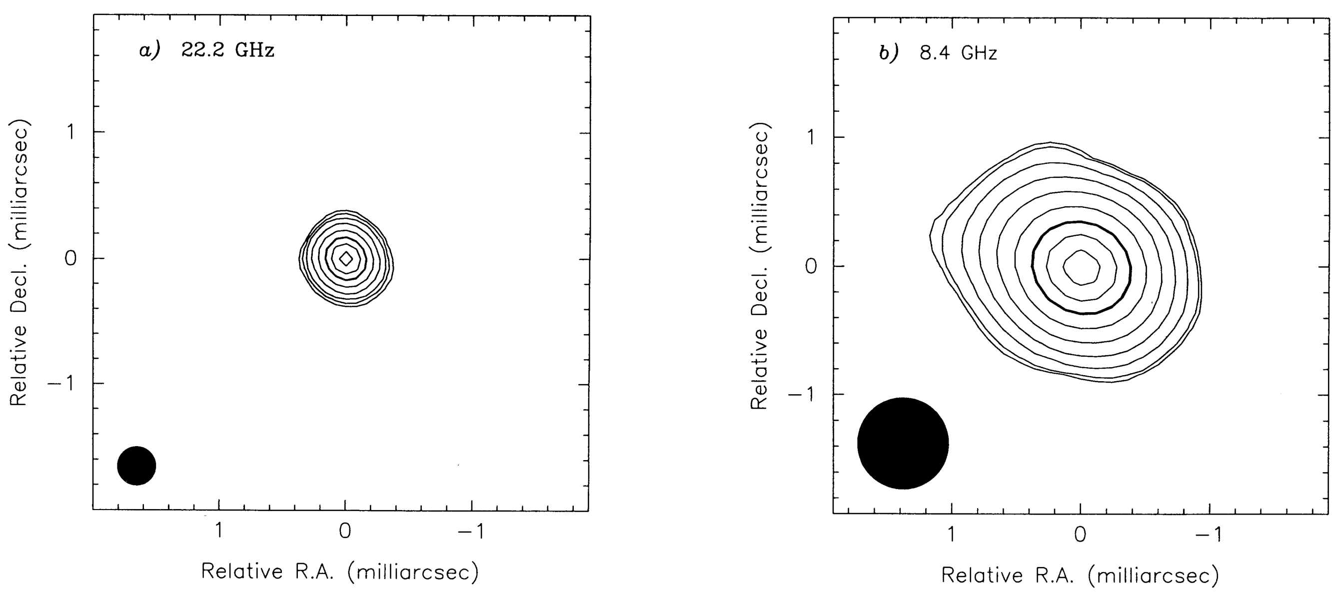

FIG. 1.—Central portion of the CLEANed images of the core of M81. The FWHM of the restoring beam is shown at the lower left. (*a*) An image at 22.2 GHz, using the data taken on April 27. Contours are at 3, 5, 8, 16, 30, **50**, 70, and 90% of the peak flux density, and the FWHM of the circular restoring beam is 0.30 mas. (*b*) An image at 8.4 GHz, using data taken on both May 17 and June 27. Contours are at 1.6, 2, 4, 8, 16, 30, **50**, 70, and 90% of the peak flux density, and the FWHM of the circular restoring beam is 0.70 mas. The rms of the background was 0.53% of the peak flux density.

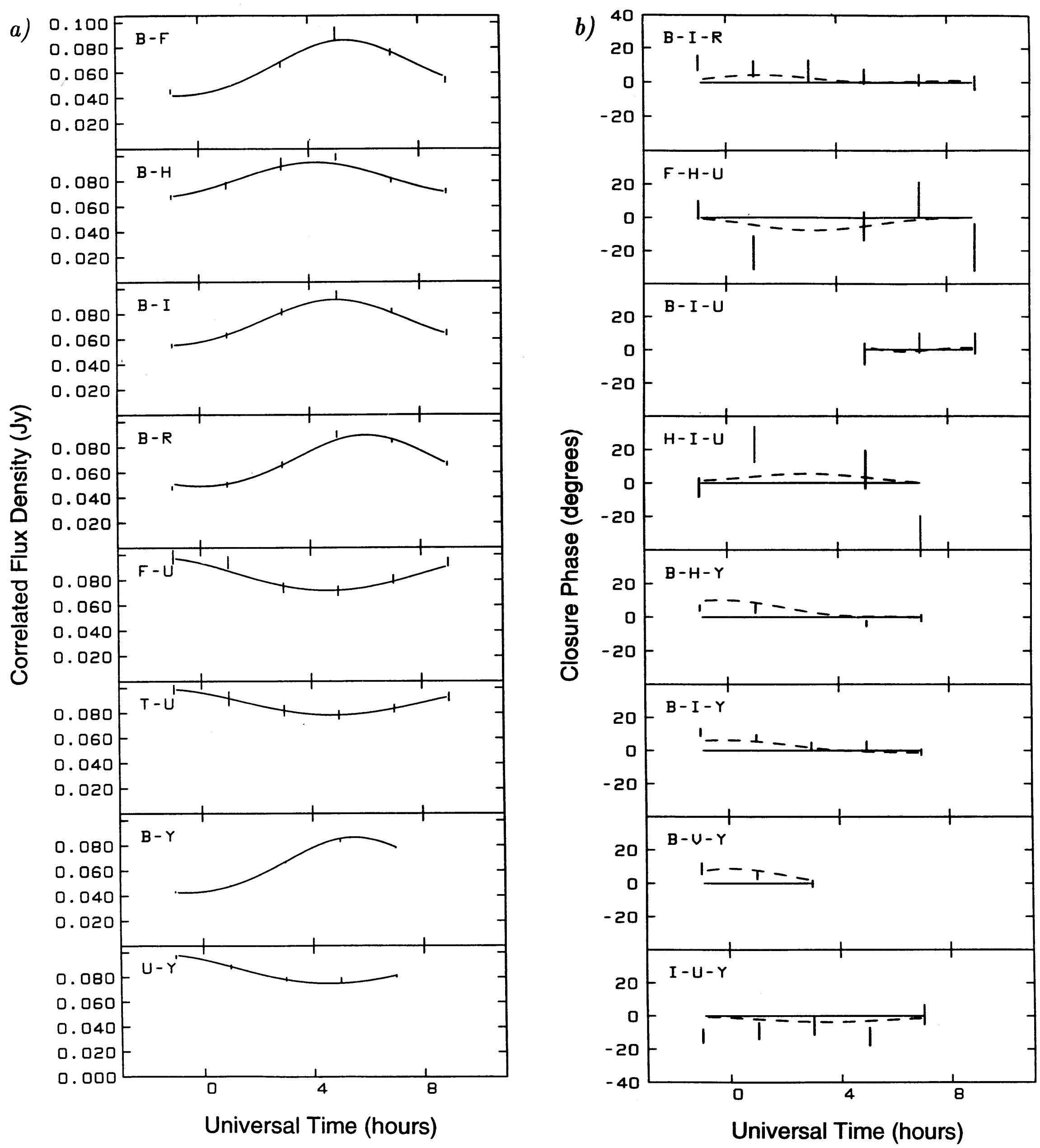

FIG. 2.—(*a*) Correlated flux densities for the longest baselines and (*b*) closure phases for a representative sample of large antenna triangles from the 8.4 GHz data of M81 taken on May 17. Uncertainties shown are calculated solely from the number of bits correlated. For the station codes see Table 1. The solid line represents the best-fit elliptical Gaussian model. The dashed line in (*b*) represents a possible "core-jet" model (see text). The corresponding line for the correlated flux densities is not drawn in (*a*), since it matches almost exactly the solid line from the elliptical Gaussian model. This core-jet model is characterized as follows: the core component is a point source with a flux density of 0.03 Jy; the jet component is an elliptical Gaussian with a flux density of 0.08 Jy at a radius of 0.1 mas and a p.a. of 57°. It was constrained to be elongated at the same p.a. The FWHM of its major axis is 0.6 mas, and the ratio between the minor and the major axis is 0.4.

generated statistically independent UV data points, which simplified the calculation of the number of degrees of freedom in the error calculations below, but also limited our field of view of about 4 beamwidths (25% time-smearing correlation losses). In all cases, however, the source is smaller than the beam, so time-smearing correlation losses are relatively unimportant. The model fitting and self-calibration process was then iterated to convergence with time-varying antenna gain factors. For the 14.9 and 5.0 GHz observations, there were considerably fewer data points, so we did not average the data and fitted only constant antenna gain factors. Below, we derive uncertainties for these model parameters that take into account the uncertainties in the derived antenna gains, whether they be time varying or not.

If we calculate the uncertainties of the amplitudes and phases solely from the number of bits correlated, the reduced chi square, χ_ν^2, of the final elliptical Gaussian fit ranges from 1.1 for the 14.9 GHz data to ~2.5 for the 8.4 GHz data. The fact that such a value for χ_ν^2 is larger than unity is probably due either to an inadequate model representation of the true source structure or to an underestimation of the data uncertainties. Since the CLEAN maps reveal no complicated structure, it is more likely that the true uncertainties of the data are larger, by a factor of up to 1.6, than those taken from the number of bits correlated. Relatively small coherence losses, estimated to be a few percent, could account for such factors. In deriving our error estimates of the model parameters, we scaled the data uncertainties so that the best-fit χ_ν^2 is equal to 1.

Because the estimates of the model parameters are likely to be correlated with the estimates of the antenna gains, we need to derive uncertainties in the model parameters which include possible contributions from the uncertainties in the antenna gains, since the latter are also free parameters. Even small correlations need to be taken into account, since we have only four model parameters but up to 50 antenna gain parameters in the case of time-varying gains. We changed each model parameter in steps, solved in each step iteratively for the remaining model parameters and the antenna gains, and monitored the change of χ_ν^2.

More specifically, let the best-fit value of a model parameter x be x_0. We then scaled the data uncertainties so that for this best fit the sum of the squared residuals would be $\chi_0^2 = \nu$, where ν is the number of degrees of freedom (ν = number of visibility amplitudes + number of phase closures − number of antenna gain values − number of model parameters). We held x fixed at value: $x_0 + \Delta x$. Again, we found the best fit, allowing all the *other* parameters to vary and converge with several iterations of self-calibration. We take the 1 σ uncertainty (1 standard error) in parameter x as that Δx which caused χ^2 to increase to $\chi_0^2 + 1$. The resulting estimates of the model parameters and their errors are given in Table 2.

Since the procedure we used fits the amplitudes and the closure phases rather than the complex visibilities, a noise bias will be present. However, this bias is small and does not significantly affect the sizes and ellipticities that we derived for the source. We estimated this bias as follows: we replaced the observed visibilities with ones derived only from the model. Then, we added pseudorandom Gaussian noise with an amplitude consistent with the χ^2 from the best-fit model. A new model was then fitted to these pseudodata, and the distribution of the derived parameters compared to the parameters of the original source model over several realizations. The resulting scatter of the parameters is consistent with our derived uncertainties. The noise bias in our derived parameters is considerably smaller than the uncertainties.

At 22.2 GHz, we find that the angular size (FWHM) of the nuclear source is 0.18 mas along the major axis and less than approximately half of that along the minor axis. At the distance of M81 of 4 Mpc, this angular size corresponds to a linear size of only 700 AU along its major axis. No other nuclear source, apart from Sgr A*, has ever been found to be that compact. In Figure 3 we plot the length of the major axis and its position angle (p.a.) as a function of frequency, and compare our results to those of B82. The size is clearly dependent on observing frequency, increasing by a factor of ~4 from 22 to 5.0 GHz. B82 found a comparable result for data at 8.3 and 2.3 GHz.

Our size estimates at 8.4 GHz agree with the estimate of B82 at 8.3 GHz to within 1 σ, consistent with no structural evolution during the 12 years between the observations. Including B82's size measurements, a weighted least-squares power-law fit shows the length of the major axis to be equal to $(2.5 \pm 0.3\ \mathrm{mas})(\nu/1\ \mathrm{GHz})^{-0.80 \pm 0.05}$, with the uncertainties again being standard errors. Our p.a. estimates at 8.4 GHz also agree with the 8.3 GHz p.a. obtained by B82 to within 1 σ. A weighted least-squares fit to our and B82's data gives p.a. = $(88 \pm 4)^\circ - (35 \pm 5)^\circ(\log \nu/1\ \mathrm{GHz})$.

Most of the closure phases are equal to zero within the uncertainties. However, in our most sensitive observations on 1993 May 17 at 8.4 GHz with the best combination of high signal-to-noise ratio and good *u-v* coverage, the closure phases from the largest antenna triangles show small but significant deviations from zero (see Fig. 2*b*). These deviations suggest that the source is asymmetric. To model these deviations, we chose, in analogy to other compact radio sources, a two-component "core-jet" brightness distribution model. The "core" consisted of an unresolved point source and the "jet" consisted of an elliptical Gaussian, elongated at the same p.a. that it was displaced from the origin. A more complicated model is not warranted, since the details of this model lie on spatial scales smaller than our diffraction-limited beam. This model provides a significantly better fit to the large triangle closure phases than a single Gaussian component fit (Fig. 2*b*). The quality of the fit to the amplitudes remained unchanged. Unfortunately, the data do not allow a unique determination of the "core-jet" parameters, but all models have the "jet"

TABLE 2

Summary of the Model-fitting Results[a]

Session	Telescopes[b]	Frequency (GHz)	Beam[c] (mas)	Total Flux Density[d] (mJy)	Major Axis[e] (mas)	Axis Ratio (Minor to Major)	Position Angle
Apr 27	BFGHILMPRTUVYX	22.235	0.25	118 ± 6	0.18 ± 0.02	$0.4^{+0.2}_{-0.1}$	$36^\circ \pm 6^\circ$
May 17......	DFHIMRTUY	22.235	0.29	121 ± 6	0.16 ± 0.04	$0.0^{+0.4}_{-0.0}$	43 ± 10
Jun 27.......	FIPRTUVX	14.867	0.66	...	0.31 ± 0.04	$0.4^{+0.1}_{-0.4}$	48 ± 7
May 17......	BCFHIPRTUVY	8.417	0.69	118 ± 8	0.46 ± 0.01	$0.44^{+0.04}_{-0.05}$	57 ± 2
Jun 27.......	FHIPRTUVX	8.417	0.92	...	0.43 ± 0.07	$0.4^{+0.2}_{-0.4}$	57 ± 8
Jun 27.......	FHIPRTUVX	4.987	2.0	...	0.70 ± 0.12	$0.0^{+0.3}_{-0.0}$	62 ± 8

[a] See text for a description of the model-fitting procedure. Uncertainties are standard errors, 1 σ, and allow for both random errors in the data and systematic gain variations.

[b] Participating telescopes; see Table 1 for codes.

[c] The FWHM of a Gaussian fit to the naturally weighted beam.

[d] Flux density values determined from simultaneous VLA imaging using 3C 286 as a flux calibrator, with beam sizes (FWHM) of 0".5 and 1" at 22.2 GHz, and 2".5 at 8.4 GHz.

[e] FWHM of an elliptical Gaussian fit to the data.

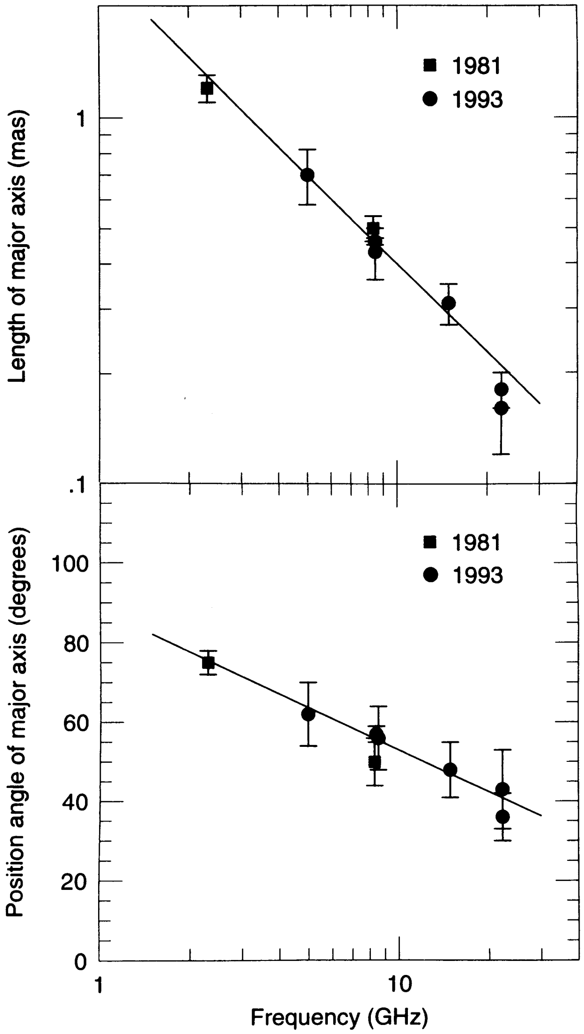

FIG. 3.—Length (FWHM) and p.a. of the major axis as a function of observing frequency. Lines indicate weighted least-squares fits. The 1993 data are from this paper, and the 1981 data are from B82.

with a surface brightness lower than that of the core and located northeast of the core. A model with the "jet" to the southwest of the core would produce sign-reversed closure phases inconsistent with the observations. We conclude that there is significant asymmetry in the core of M81, with the surface brightness being lower toward the northeast.

4. DISCUSSION

Our images of the nuclear region of the spiral galaxy M81 have revealed that the extremely compact core is slightly asymmetrical about its center, suggesting an extension toward the northeast. The size along its extension is only 700 AU at 22.2 GHz and, as is common in compact extragalactic sources, varies with frequency as $\nu^{-0.8}$ between 22.2 and 2.3 GHz in our case. The orientation of the extension is also frequency dependent and changes from 40° to 75° for the same frequency range.

We find that no significant change has occurred in the size or orientation since the last VLBI observations of this source 12 yr earlier (B82). In particular, the nominal expansion velocity of the core region along the major axis is -3 ± 3 μas yr^{-1}, or, at a distance of 4 Mpc, -60 ± 60 km s^{-1}.

Terlevich & Melnick (1985) and Terlevich et al. (1992) have discussed the activities in the center of galaxies in terms of starburst and supernova models. For M81 such models are not appropriate because the core has a brightness temperature of (2–3) $\times$ 10^{10} K (at 8.4 GHz), a very small size, and lacks significant structural variability. In particular, if the core emission were due to supernovae, then only very few supernovae would be required to account for the relatively low luminosity of the core of $\sim 10^{37.5}$ ergs s^{-1} (for $\nu < 100$ GHz). But with only a small number of supernovae, the effects for the expansion of individual supernovae (with velocities up to 20,000 km s^{-1}) should be observable. In fact, SN 1993J in M81 had a peak luminosity almost as large as that of the core and expanded at a rate of ~ 3 μas day^{-1} (Bartel et al. 1994), more than 300 times faster than what is indicated by the 2 σ upper for the core. These considerations strongly argue against a starburst or a supernova model for M81's core, and instead favor, analogous to other AGNs, a black hole with an accretion disk and a jet.

The apparent size of the nuclear source depends strongly upon the observing frequency. This dependence cannot be due to scattering in our Galaxy because our VLBI observations of SN 1993J (Bartel et al. 1994) show no such effect. It is very unlikely to be due to scattering within M81 either, because scattering would produce an approximately ν^{-2} dependence of the apparent size and, given the relatively large distance to M81, an unreasonable amount of scattering would be required (see Backer 1978) to reproduce our observed source sizes. Instead, the frequency dependence is intrinsic to the source.

The apparent size of a uniform optically thin source is not expected to depend on frequency, so we consider here (see the arguments advanced in B82) a nonuniform synchrotron self-absorbed source, with a magnetic field $\boldsymbol{B}(r) \propto r^{-m}$. The properties of such sources have been examined by Marscher (1977). Adopting B82's value for the spectral index in the optically thick regime ($\alpha = +0.2$, $S_\nu \propto \nu^\alpha$, S_ν: flux density at frequency ν), we get $m = 1.7 \pm 0.8$. However, the source is not spherically symmetric, so this symmetrical model is not expected to apply in detail. The source has also been shown to be variable (Crane et al. 1976; Bartel, Bietenholz, & Rupen 1995), which could limit the accuracy obtainable by combining measurements at different epochs. We find, however, no evidence of changes in structure since the B82 observations of over a decade ago.

Although our resolution is not high enough to claim unambiguous detection of a jet in the core of M81, a bent steep-spectrum jet seems the most reasonable interpretation of the change in the p.a. by $\sim 35°$ over the length scale from 700 to 4000 AU, corresponding to the frequency range from 22.2 to 2.3 GHz. M81's rotation axis, as derived from H I observations (Rots & Shane 1975), has a p.a. of 62° $\pm$ 3° which lies in the middle of the observed nuclear source p.a.'s but is significantly different from the largest and the smallest scale p.a.'s that we determined. In particular, the discrepancy with respect to the smallest scale p.a. (38° $\pm$ 5° at 22.2 GHz) indicates either that the jet axis *is* aligned with the galaxy's rotation axis and considerable bending occurs on scales even smaller than 700 AU, or that the jet axis is *not* aligned with the galaxy's rotation axis.

We compare the core of M81 with the compact source in our Galaxy's center, Sgr A* (for a review see Backer 1994). The latter also shows a size that decreases with observing frequency (e.g., Backer 1994; Krichbaum et al. 1993; Marcaide et al. 1992), but with the size being proportional to ν^{-2} (at least for frequencies below 20 GHz), which is thought to be the result of scattering. The linear size of Sgr A*, however, is less than 15 AU at 22.2 GHz, which is smaller than that of the core of M81 at this frequency (300–700 AU). The radio luminosity of Sgr A* is also 10^4 times less than that of the core of M81.

Assuming that projection effects are not large, the fact that the p.a. and the size at 8.4 GHz have not changed significantly over the past decade, while the source size at that frequency is only ~ 10 light-days, makes any explanation of the bend in terms of ballistic precession unlikely, unless $v \lesssim 1000$ km s^{-1}. This would be inconsistent with unified models of AGNs (see, e.g., Antonucci 1993 for a review) which predict that the speed of the bulk motion should be nearly c in all cases. If the jet speed *is* $\sim c$, then it must flow along an almost steady state channel, otherwise we would observe structural variability. Such behavior is observed in other VLBI sources (e.g., Roberts & Wardle 1994; Marcaide et al. 1994). If such a channel is associated with a precessing engine, its precession period must be longer than a few hundred years.

If we interpret our observations as indicating a nuclear jet, then the radio core of M81 much resembles a very compact version of what is typically seen in larger, brighter AGNs: a flat or inverted spectrum core and a steeper spectrum jet. Falcke, Mannheim, & Biermann (1993) have adopted the unconfined jet model of Blandford & Königl (1979) for Sgr A*. By applying this model to the core of M81, we find that the *minimum* accretion rate required to produce the observed radio-flux density is $\sim 10^{-5.5}$ $M_\odot$ yr^{-1}, again assuming that projection effects are not large. This is consistent with the accretion rate of $\dot{M} \leq 10^{-4}$ to 10^{-3} $M_\odot$ yr^{-1} that Fabbiano (1988) determined by fitting an accretion disk model to the UV and X-ray spectrum of M81.

The above jet model (Blandford & Königl 1979), with the accretion rate specified, predicts the observable length of the jet. In order to accommodate both the observed flux density from the jet and our observed projected jet length (i.e., 700 AU at 22.2 GHz), we find that the angle, i, between the jet and our line of sight cannot be small and is probably $\gtrsim 30°$. This implies that we are *not* looking directly down the jet. If we were, the jet would be either brighter or shorter than observed. It further implies that the observed sweep of the core p.a. of 35° must be due to relatively large intrinsic bends in the jet and cannot be explained by small intrinsic bends of, for example, only a few degrees magnified by projection.

The core of M81 has a spectrum showing broad emission lines resembling that of a Seyfert I galaxy (Filippenko & Sargent 1988). According to the unified models for AGNs, this would imply that the nuclear source is nearly face-on, and that we can see directly into the broad-line region (BLR). However, analogous to brighter Seyfert galaxies, one would then expect to see strong variability in the broad-line component of the nuclear emission, which is not observed (Filippenko & Sargent 1988). Also, in this picture the inclination angle of the jet would be rather small, in contrast to $i \gtrsim 30°$ suggested above. For $i \gtrsim 30$, we may be seeing reflected instead of direct BLR emission, which may also explain its lack of variability, as suggested by Antonucci (1993).

Regardless of orientation, it is somewhat surprising that no change in structure is evident over 12 yr. Ghisellini et al. (1993) found that 39 out of 105 bright VLBI sources exhibited superluminal motion. A component moving at an apparent speed of $\sim c$ would reach the edge of our field of view in ~ 1 yr. The lack of any such component implies that the ejection frequency is probably less than several per year. Alternatively, the ejected components would just fade below our detection limit within an angle of 0.2 mas of the core, as expected if the unconfined model of Blandford & Königl (1979) is applicable.

The properties of the core of M81 seem to be intermediate between those of the core of the Galaxy and those of much larger, more active AGNs. Models comprising a central black hole with an accretion disk and an unconfined jet seem to be able to account approximately for the observations. Such models have had some success in accounting for the properties both of far more luminous AGNs and of the far less luminous source at the Galactic center. Compact radio-emitting cores with spectral power equal to that of the core of M81, 2×10^{20} W Hz^{-1}, are not uncommon. Hummel, van der Hulst, & Dickey (1984) found that 12% of Sb spirals have cores with radio spectral power greater than 10^{20} W Hz^{-1} (see Wrobel & Heeschen 1991). This suggests a continuum of AGN activity ranging from the more powerful, and usually more distant, AGNs to the relatively weak source at the Galactic center. The core of M81, being in the middle of this continuum, has the advantage of being quite close. It presents a unique opportunity to study a low-power AGN at high angular resolution.

We thank K. I. Kellermann and an unknown referee for valuable and useful comments on an earlier version of this paper. Research at York University was partly supported by NSERC. NRAO is operated under license by Associated Universities, Inc., under cooperative agreement with NSF. The NASA/JPL DSN is operated by JPL/Caltech, under contract with NASA.

REFERENCES

Antonucci, R. 1993, ARA&A, 31, 473
Backer, D. C. 1978, ApJ, 222, L9
———. 1994, in Compact Extragalactic Radio Sources, ed. J. A. Zensus & K. I. Kellerman (Socorro: NRAO), 149
Bartel, N., et al. 1982, ApJ, 262, 556
———. 1994, Nature, 386, 610
Bartel, N., Bietenholz, M. F., & Rupen, M. P. 1995, Proc. Natl. Acad. Sci., 92, 11374
Bietenholz, M. F., et al. 1994, in Compact Extragalactic Radio Sources, ed. J. A. Zensus & K. I. Kellermann (Socorro: NRAO), 109
Blandford, R. D., & Königl, A. 1979, ApJ, 232, 34
Crane, P. C., Giuffrida, T. S., & Carlson, J. B. 1976, ApJ, 203, L113
de Bruyn, A. G., Crane, P. C., Price, R. M., & Carlson, J. B. 1976, A&A, 46, 243
Elvis, M., & Van Spybroeck, L. 1982, ApJ, 257, L51
Fabbiano, G. 1988, ApJ, 325, 544
Falcke, H., Mannheim, K., & Biermann, P. L. 1993, A&A, 278, L1
Filippenko, A. V., & Sargent, W. L. W. 1988, ApJ, 324, 134
Freedman, W. L., et al. 1994, ApJ, 427, 628
Ghisellini, G., Padovani, P., Celotti, A., & Marschi, L. 1993, ApJ, 407, 65
Hummel, E., van der Hulst, J. M., & Dickey, J. M. 1984, A&A, 134, 207
Kellermann, K. I., Shaffer, D. B., Pauliny-Toth, I. I. K., Preuss, E., & Witzel, A. 1976, ApJ, 210, L121
Krichbaum, T. P., et al. 1993, A&A, 274, L37
Marcaide, J. M., et al. 1992, A&A, 258, 295
———. 1994, in Compact Extragalactic Radio Sources, ed. J. A. Zensus & K. I. Kellermann (Socorro: NRAO), 141
Marscher, A. P. 1977, ApJ, 82, 781
Napier, P. J., Bagri, D., Clark, B. G., Rogers, A. E. E., Romney, J. D., Thompson, A. R., & Walker, R. C. 1994, Proc. IEEE, 82, 658
Peimbert, N., & Torres-Peimbert, S. 1981, ApJ, 245, 845
Roberts, D. H., & Wardle, J. F. C. 1994, in Compact Extragalactic Radio Sources, ed. J. A. Zensus & K. I. Kellermann (Socorro: NRAO), 201
Rogers, A. E. E., et al. 1983, Science, 219, 51
Rots, A. H., & Shane, W. W. 1975, A&A, 45, 25
Rupen, M. P., et al. 1994, in Compact Extragalactic Radio Sources, ed. J. A. Zensus & K. I. Kellermann (Socorro: NRAO), 103
Shepherd, M. C., Pearson, T. J., & Taylor, G. B. 1994, BAAS, 26, 987
Terlevich, R., & Melnick, M. 1985, MNRAS, 213, 841
Terlevich, R., Tenorio-Tagle, G., Franco, J., & Melnick, J. 1992, MNRAS, 255, 713
Wheeler, J. C., et al. 1993, ApJ, 417, L71
Wrobel, J. M., & Heeschen, D. S. 1991, AJ, 101, 148